Deliverable D2.1.1

New actuators for the robot companion

Deliverable due date: 31 October 2013	**Actual submission date: 31 October 2013**
Start date of project: 1 November 2011	**Duration: 48 months**
Lead beneficiary for this deliverable: IIT	**Revision: 0.#/1.#/Final**

Nature: P	Dissemination Level: PU
R = Report P = Prototype D = Demonstrator O = Other	PU = Public PP = Restricted to other programme participants (including the Commission Services) RE = Restricted to a group specified by the consortium (including the Commission Services) CO = Confidential, only for members of the consortium (including the Commission Services)

Deliverable summary

One of the aims of WP2 is to pursue research into the development of actuation components and robot body technologies for a new generation of robots that can safely co-exist and co-operate with people, and at the same time get much closer to human performance than is possible with current robots. In particular, WP2 explores new actuators, sensors, and systems integrating the "robot companion" vision central to SAPHARI project. This report accompanies D2.1.1 - New actuators for the robot companion (Prototype) and presents the design and implementation of the variable impedance actuator (VIA) developed by the Consortium in WP2 during the first two years of activity. The focus is on the actuators developed using classical electromechanical components. The report introduces the working principles of the actuators and presents CAD documentation details and real assembly images to demonstrate how each principle was finally realized into a prototype. The report is divided into two parts. The first introduces the developments of the variable stiffness units while the second part presents the units developed in Task 3.2 (Actuators with Adjustable Damping).

Table of contents

1 Main results

To meet the objective of D2.1.1 the work in WP2 was focused along several lines of research. These activities were related to development of new actuation mechatronic components towards the realization of variable impedance actuation devices. Starting from prototype actuators developed in previous EU projects e.g. VIACTORS upgrades and improvements on some of these existing modules were investigated. Additional new concepts and mechanisms for the realization of variable impedance actuator groups were also studied, identified and built. In overall the achievement highlights of D2.1.1 include:

- Two new variable damping prototypes and improvements on an existing solution.
- New variable stiffness actuators implementing different multiday kinematics such as shoulder or knuckle joints.
- New conceptual implementations of VSA units based on non-circular gear transmission.
- The evaluation of the performance of the above variable impedance joints.

In detailed a fluid based damper unit to form an add-on module for the VSA-Cube actuator was designed. The basic goal behind the development of this actuator was to obtain a modular damping unit that can be integrated with the VSA-CubeBot system (e.g. in the shoulder), and provide the capability of changing the damping value for the VSA joint [1].

The Piezo-Actuated-based variable damping units developed in task 2.1 were used to form a 4DOF manipulator arm. A roll-pitch-roll "spherical" joint made of the series longitudinal-transverse-longitudinal forms the shoulder of the manipulator [2-4].

Following this, a damping actuator based on a linear drive clutch mechanism was realized to provide improved performance over the piezo-actuated-based. In this actuator a motorized drive technology instead of piezoelectric actuation was employed for the implementation of the actuation of the new VPDA system to provide higher levels of grip and damping [5].

Regarding the variable stiffness actuation developments prototypes of multi degrees of freedom VIA, suitable, in its first release, for an implementation of a robotic wrist were realized. Further studies could be useful for an extension/reconfiguration as, for example, a robotic shoulder. The main idea behind this prototype is the realization of a system with which is possible to control, simultaneously, the position and the stiffness characteristics of two degrees of freedom joint.

Furthermore, the VSA-Gear implementation, which can be classified as an Agonist-Antagonist Variable Stiffness Actuator realized through the adoption of non-circular gear transmission, was studied. Main

advantage of the implementation is the simplicity of the mechanism and the ability to easily adapt the actuator properties with minimum modifications in the actuator components

Finally, the functionality and performance of some of the above actuator prototypes were studied and demonstrated in several experiments [6-8]

Figure 1 and 2 summarize the achievements of deliverable D2.1.1 by presenting the most relevant VIA prototype devices and integrated systems developed during the first two years of the project. The relevant scientific dissemination produced from this work until now is also reported in section 2.
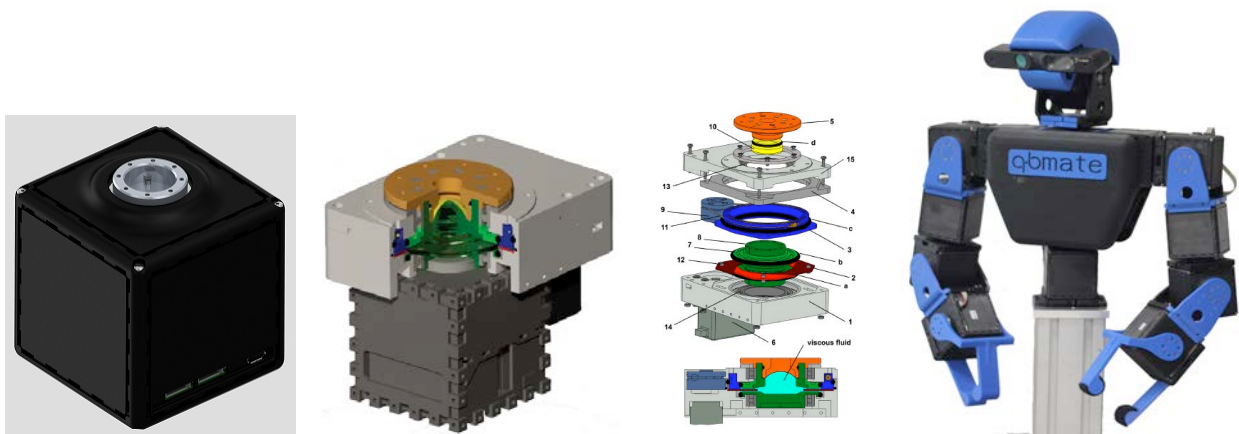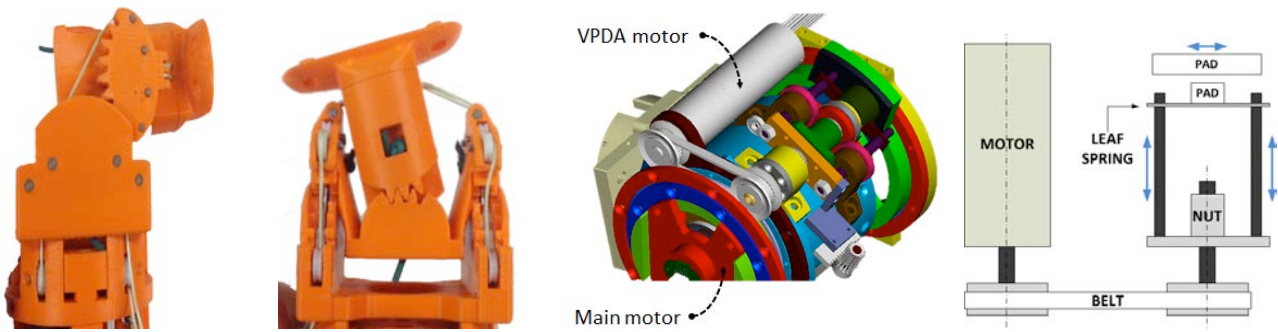

a)   Cube actuator and the add-on variable damping module
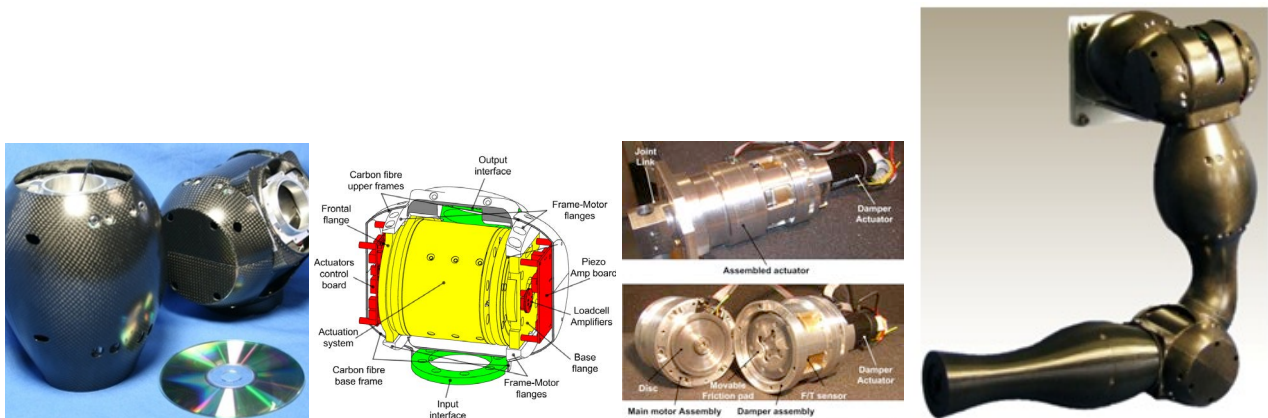
b)   The revised VPDA and the new motorized clutch based variable physical damping concept proof prototype

Figure 1.1 Examples the VIA actuation components developed within WP2 during the first two years of the project.

a) Multidof VIA implementations and the new motorized clutch based variable physical damping unit
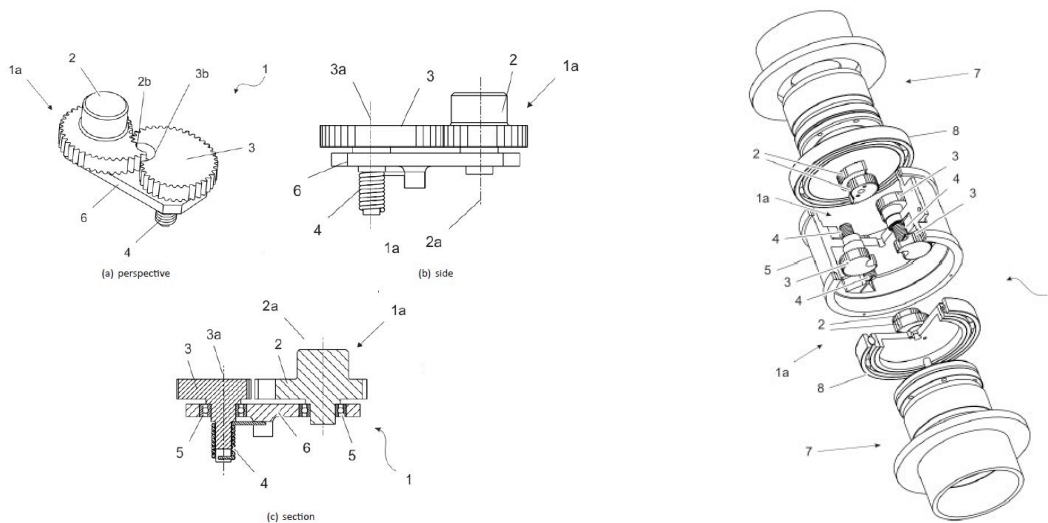
b) The VSA-Gear, conceptual implementation of an Agonist-Antagonist Variable Stiffness Actuator, realized through the adoption of non-circular gear transmission

Figure 1.2 Additional examples of the VIA actuation components developed within WP2 during the first two years of the project.

2 VIA Implementations

Variable Impedance Actuation (VIA) is a relatively recent technology with multiple different implementation principles, each having its own advantages and disadvantages. One of the main objectives of WP2 was to develop further VIA technologies (mainly those proposed in the past by some of the members of the consortium, but also by exploring new ideas and principles) and to integrate them in upper-body robotic subsystems. Along this direction, different variable impedance actuators with very unique and distinctive implementations were implemented by the Consortium based on a diverse range of physical principles and mechanisms.

In particular, two main VIA implementations were explored, namely:

i)   the variable stiffness approach

ii)   and the variable damping implementation

The first approach makes use of variable stiffness actuators (VSA) to regulate the stiffness component of the impedance while the damping component of the impedance is actively controlled by the main motor. The second variable impedance actuator principle instead integrates series elastic actuation with variable physical damping units to realize robots where damping is passively controlled and stiffness is actively regulated. The development of these alternative systems allows validating the performance of different VIA solutions according to the WP2 objectives, and enables also a rigorous experimental evaluation of control and estimation algorithms developed in WP3 on platforms of different nature. The rest of this deliverable is structure as follows; section 3 presents the design and implementation of variable stiffness actuators while section 4 introduces the development on the variable damping units.

3 Variable Stiffness Actuation

Recent robotic research recognizes the advantages that Variable Stiffness Actuators which would yield to a new generation of robots, rendering them adapt to many different tasks of everyday life provide improved physical interaction behaviours and responses. The developments in this area included the study of two novel Variable Stiffness Actuator designs. The first is based on the Non-circular gear based variable stiffness actuation principle while the second deals with the implementation of multi-degree of freedom VSA joints.

3.1 Variable stiffness actuation based on Non-circular gear transmission

Recent robotic research recognizes the advantages that Variable Stiffness Actuators which would yield to a new generation of robots, rendering them adapt to many different tasks of everyday life. In this work, a novel Variable Stiffness Actuator design is proposed, in which the elastic stiffness characteristic is obtained thanks to proper design of non-circular gears. This offers the important advantage of allowing an easy method for the customization of the non-linear characteristic of the VSA mechanism while keeping a fixed actuator structure. One of the most important components of the robot is definitely identifiable in the actuator. In recent years, in order to improve the safety and the working precision of these robots, various mechanisms called Variable Stiffness Actuators (VSA) which are characterized by nonlinear elastic characteristic have been designed in order to obtain actuators capable of changing their stiffness and ensuring, at each instant, excellent quality of machining and high safety.

Most of the design of such mechanism present the drawback that they are particularly complex in realization. In particular, this complexity is due to the high number of components needed to implement the nonlinear elastic characteristic, which leads to high realization costs. A further problem of such non-linear elastic mechanisms is represented by their poor adaptability. In fact, the modification of the mechanical stiffness characteristic requires, when possible, the replacement of almost all the components through the execution of complicated operations. This drawback usually pairs with a limited range of obtainable stiffness values.

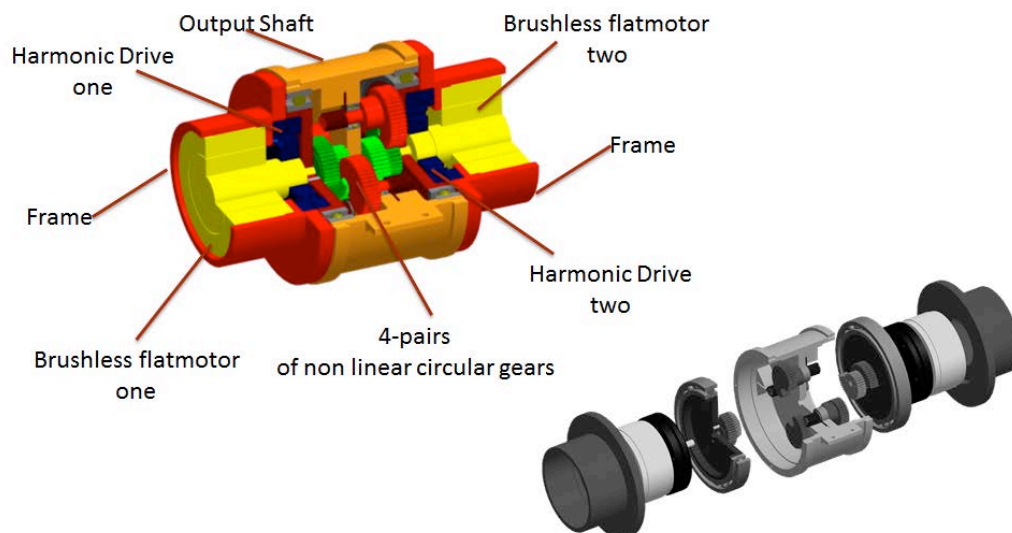**Figure 3.1** The VSA-Gear, an Agonist-Antagonist Variable Stiffness Actuator, realized through the adoption of non-circular gear transmission. Section view of the full actuator, complete with the two torque motors.

Figure 3.1 presents a nonlinear elastic mechanism with an easily programmable characteristic capable of substantially obviating the mentioned drawbacks. It is believed that such a solution can be achieved with

the adoption of a non-linear elastic mechanism designed by using non-circular gears. In the following a possible design, whose implementation is forecast in the near future, is presented.

The characteristics and advantages of the device are here described, with reference to the accompanying drawings. Figure 3.2(a), (b) and (c) show different views of a single non-linear elastic transmission system (1), implemented with a non-circular gears transmission. The transmission system includes a first gear (2) adapted to be connected to the first element and defining a first axis of rotation (2a) and a second gear (3) which is engaged with (2) and connected to output rotation axis(3a). Finally a spring (4) is connected with (3) and the frame (6).
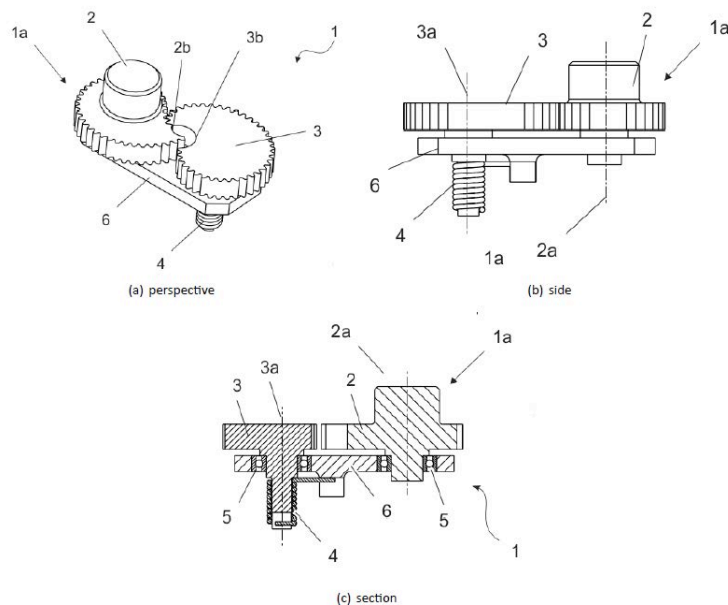
Figure 3.2 Non-circular gear non-linear stiffness mechanism. The particular gear profile implements an exponential torque-deflection profile.

These toothed wheels (2) and (3) can present a variety of profiles, elliptical, spiral, etc. The device shown in figures has been designed such to present an exponential mechanical stiffness characteristic, in which the output torque is proportional to an exponential function of the displacement.

The actuator is designed as a modular unit which can be combined to realize VSA robots, as the simple robot arm that is shown in Fig. 3.3.

Figure 3.3 The VSA-Gear Agonist-Antagonist VSA, exploded view and the realization of simple 3D arm with 3 VSA-Gear modules.

3.2 Multi degrees of freedom VIA

Another activity of the variable impedance actuation developments during the second year was the study and realization of multi degrees of freedom VIA systems, suitable, in its first release, for an implementation as a robotic wrist. Further studies could be useful for an extension/reconfiguration as, for example, a robotic shoulder. The main idea behind this prototype is the realization of a system with which is possible to control, simultaneously, the position and the stiffness characteristics of two degrees of freedom joint. In the specific prototype, in order to save space and reduce the number of actuation units, a new arrangement of motors and springs is realised. The result is a system in which the two DOFs are controlled independently, but they have in share the same stiffness characteristics. With this approach is possible to use three motors instead of four, and reduce the weight and the volume of the device.
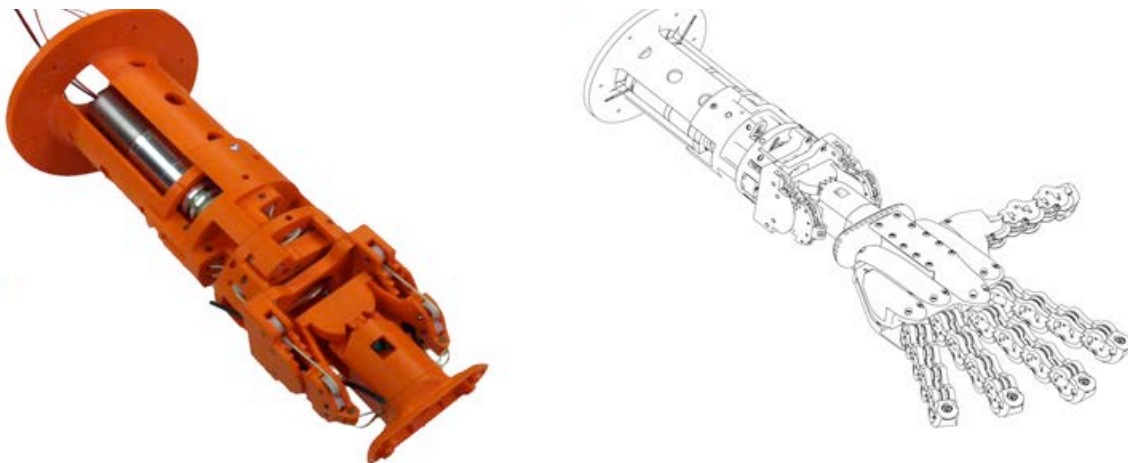

Figure 3.4 Prototype of the multi degrees of freedom VI wrist (right), 3D view (left) of the multidof wrist combined with an anthropomorphic robotic hand (Pisa/IIT SoftHand).

Figure 3.4 shows the realised prototype and a three-dimensional view of the system attached to an end-effector, like for example an anthropomorphic robotic hand. Some of the main mechanical features of the new device are related to the design of the two DOFs joint and to the arrangements of ligaments that connect and actuate the joint itself. The joint is inspired by the solution and implementation adopted on the finger joints of the Pisa/IIT Soft Hand, that is in turn an evolution of the Hillberry joint. The developed solution represents the extension of the joint of the Pisa/IIT SoftHand to a two DOFs configuration, as shown in Fig. 3.4 and 3.5.
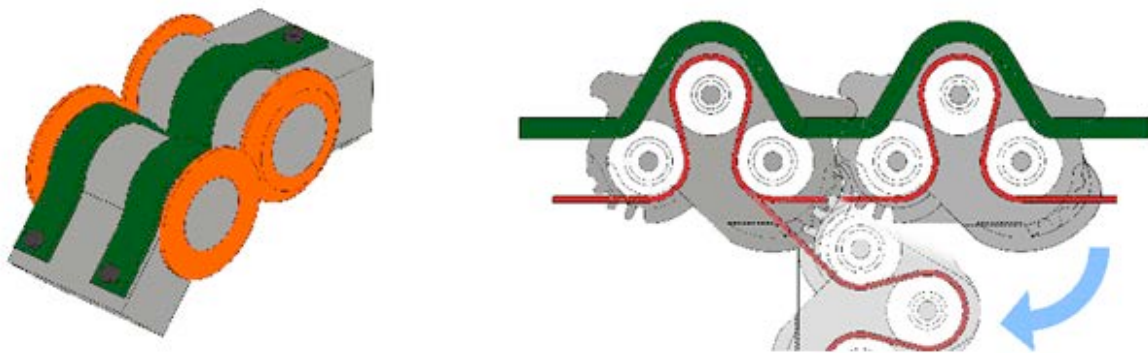
Figure 3.5 Schematic illustration of the Hillbarry Joint (right) and design of the compliant rolling-contact joint used in the interphalangeal joints of the Pisa/IIT SoftHand (left).

Figure 3.6 Range of movement of the multidof variable impedance wrist, flexion/extension (right), ulnar/radial (left).

The joint designed presents some interesting and powerful characteristics, as listed below and shown in Fig. 3.6 and 3.7:

- In the joint structure there are no screw, bolts etc. The mechanical components are linked one with another by elastic ligaments. This approach confers to the system the capability to be stretched, wrapped, and allow to the system to absorb high impact (see Figure 8).

- The range of motion is near 270°, with a kind of movement much more similar to the human behaviour with respect to a conventional rotational joint (see Figure 7).
- The system is characterized by a low friction coefficient, due to the fact that the surfaces are in a rolling contact configuration (see Figure 6).
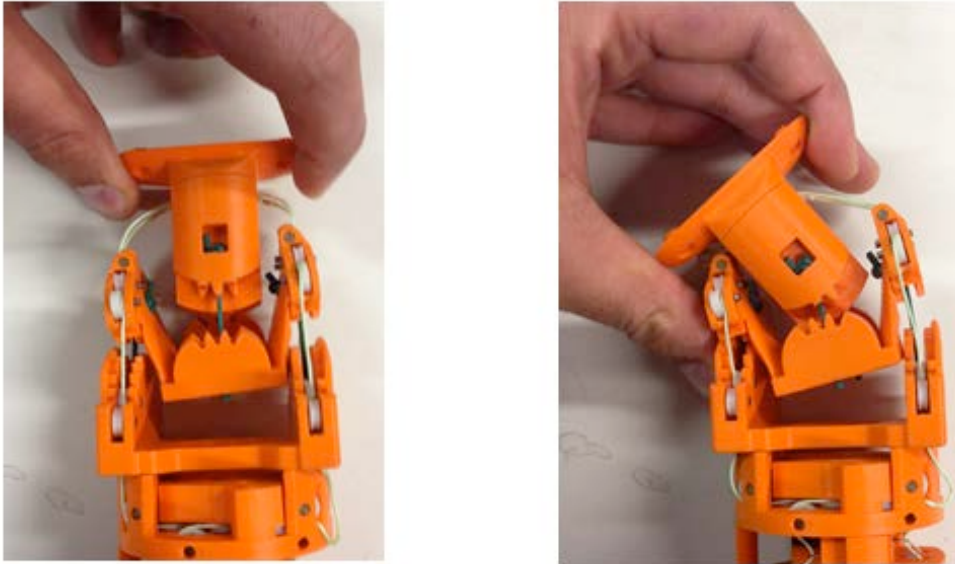

Figure 3.7 example of two different kind of disarticulation, straight t stretching (right) and lateral stretching (left).

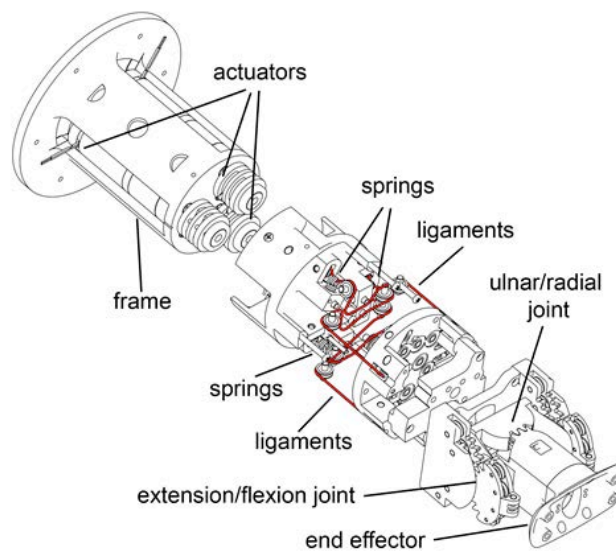The actuation system, the motors and ligaments are shown and shortly described in Fig. 3.8.

Figure 3.8 Explode 3D view of the VI wrist, in the picture highlights the main mechanical components and the actuation ligaments.

4 Variable Damping Actuation

The elasticity embedded in compliant actuators introduces dynamics which can induce oscillations with a frequency that varies on the basis of the stiffness of the joint and the inertia of the link. To supress these oscillatios the introduction of damping acton is necessary. This damping can be provided either by active , semi-active or passive solutions with he latest realized through the implentation of passive damper actuation modules. This section introduces the WP2 developments in the area of passive damping modules as actuation add-on components to complement the physical elastiity of compliiant joints of fixed or variable stiffness.

4.1 Piezo-Actuated clutch based variable damping mechanism

The CompAct[TM] – VPDA actuator, Fig. 4.1, is a series elastic actuator integrated with a clutch which is placed in parallel to the transmission compliance and is actuated by piezoelectric stack actuators[2]. Compared to the other existing compliant linear or rotary actuators the proposed unit has the ability to regulate the oscillations induced by the compliance using variable physical damping actuator (VPDA) unit [3,4]. The main work in this activity involved the revision of the compliant + VPDA actuator to realized two different modular units: the longitudinal and transversal actuation modules and consequent integration to realize a 4DOF arm [3].
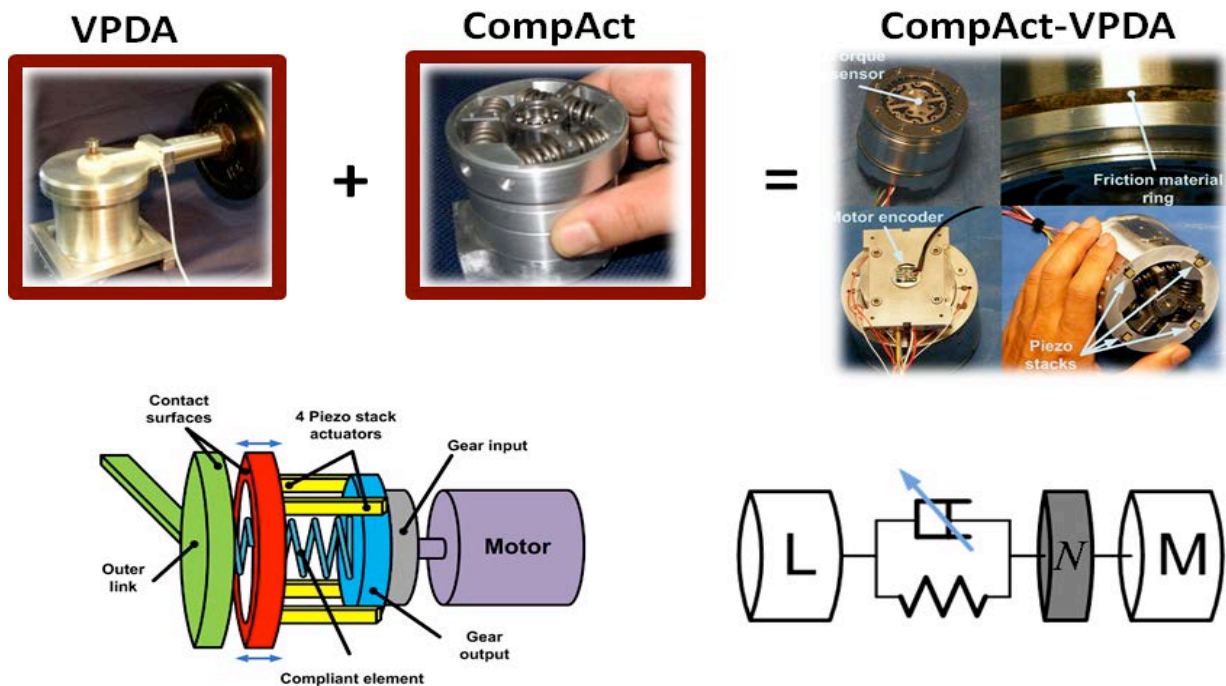

Figure 4.1 CompAct[TM] –VPDA actuator composed by the series elastic actuator CompAct[TM] and the clutch based variable damping (VPDA) unit

Modular Design Concept: the longitudinal and transversal CompAct^{TM} actuation units

Based on the modular design concept the CompAct^{TM} - VPDA actuation units were mechanically reshaped following the Longitudinal and Transverse kinematic schemes for developing a manipulator arm. To satisfy the lightweight property of the overall arm a carbon fibre frame was used in this design. The mentioned structure is used not only as frame but also as a cover preventing the human/environment to enter in contact with the mechatronics of the manipulator therefore improving its robustness and safe properties. The design of the longitudinal actuation module is shown in Fig. 4.2a. The actuation system is fixed to the carbon fibre frames in two points, i.e. at the base and front support flanges of the actuator Fig. 4.1. This is to avoid the application of thrust moments to the actuator which may result in malfunction due to the misalignment between the frictional surfaces of the damping system.

a)   b)
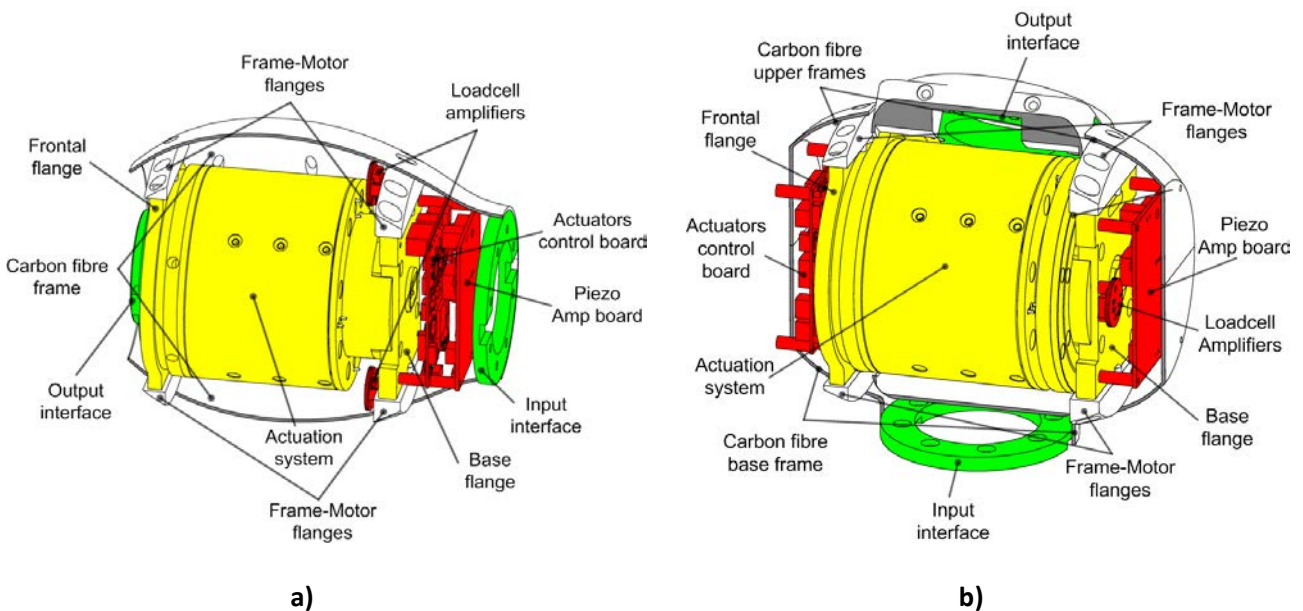
Figure 4.2 a) Open view of the longitudinal actuation module (yellow: actuation system, red: electronics, green: input-output interfaces), b) Open view of the transverse actuation module (yellow: actuation system, red: electronics, green: input-output interfaces)

The input interface is an aluminium disk which is directly connected to the frame by means of structural adhesive while the output interface is an aluminium component machined with a geometry which is the negative of that of the input disk. In the transverse configuration the frame has been designed in order to allow the replication of the kinematic configuration mentioned previously. Similarly as in the longitudinal module, the actuator is supported on both sides by means of the base and front flanges for the same reasons previously explained Fig. 4.2b. The input and output mechanical interfaces present the same geometry as that of the longitudinal module in order to fulfil the modular property and permit arbitrary

interconnections between the modules. Its specifications are reported in Table 4.1 together with those of the longitudinal module.

Figure 4.3 Longitudinal (left) and transverse (right) actuation modules.

Table 4.1 Specifications of the longitudinal and transverse actuation modules.

Parameter	Value
Gear ratio − N	100
Power	190 W
Maximum output continuous torque	40 Nm
Maximum joint velocity	10.7 rad/s (≈ 610 °/s)
Maximum rotary passive deflection	±0.18 rad
Maximum damping torque	9 Nm
Joint stiffness	188 Nm/rad
Inherent joint viscous damping	0.25 Nms/rad
Total mass of the longitudinal actuator - m_s	2.2 kg
Total mass of the transverse actuator - m_r	2.4 kg

Finally, force sensing solutions were integrated, Fig. 4.4, to sense the force applied to the clutch system by the piezoelectric stacks. Custom load cells were designed and a FEM study has been carried out to check the stress, strain and stiffness properties of the part were appropriate. In detail, the stiffness parameter is important to deal with the short stroke of the piezoelectric stacks, i.e. approximately 70μm. The results of this FEM simulation are reported in Figure 4.4.
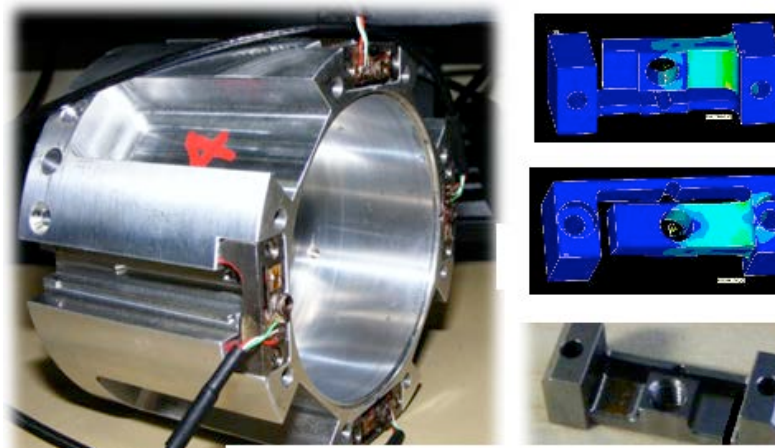
Figure 4.4 Piezo force sensors design and arrangement.

Figure 4.4 shows that the strain is approximately constant along the beam. This is obtained by means of a non-constant cross-section of the beam proportionally increasing the size of the beam moving towards its base. In this way the bending stress becomes more uniform along the beam relaxing the dimensional constraints for the placement of the strain gauge.

The actuator and its control scheme have been evaluated in several studies [5-8] and its performance has been characterized in terms basic functionality as well as in terms of performance comparison and improvement against pure series elastic joints.

4.2   Motorized linear drive clutch based variable damping mechanism

The variable damping actuator tried to address the main deficiencies of the original piezo-actuated version described in section 4.1. These include the high cost, the relative low clutching torque and the high mechanical tolerances requirements. This new actuator consists of the same main motor driving the joint but the clutch based damper mechanism in this case is controlled not by piezo stacks but by a secondary motor actuator which is shown in Fig. 4.5a. The main motor drives directly the output link, while the damper assembly provides damping to the link in the form of a controlled disc brake acting on the rare side of the joint motor shaft. In this arrangement the damper is effectively connected in parallel to the joint link with respect to ground (actuator casing). A CAD model of the actuator is shown in Fig. 4.5b and a section view in Fig. 4.6. The actuator consists of two primary sub-assemblies, the main motor assembly and damper motor assembly. The main motor assembly consists of a frameless DC motor from Kollmorgen (Model: QT-1406) with a custom casing and a custom shaft and incorporates an optical incremental encoder with 17bit resolution (Model: MicroE 5340, CE300-4). On the rare end of the motor shaft is mounted the brake disk. The brake disk is attached on the shaft with a linear joint coaxial with the shaft, which allows self-positioning and release of the disk between the stationary and movable brake pads. The stationary brake

pad is formed by the motor casing (encoder cover) on the main motor side, while the movable pad is attached on the damper motor assembly and is driven by the damper motor through the ball screw linear joint. The motor casing, the motor shaft and the brake pads are made out of aluminium while the Brake disc is made out of steel.
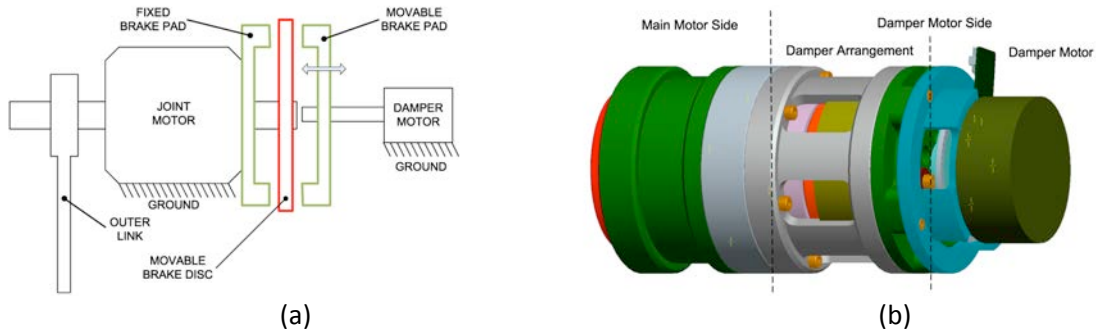

(a)   (b)

Figure 4.5 a) Conceptual schematic of the Mechanical Damper, b) 3-D view of the first Mechanical Damper prototype based on a motorized linear drive.
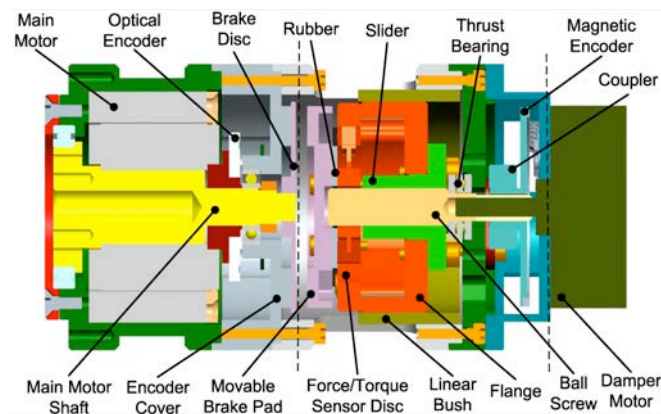

Figure 4.6 Sectional view of the Mechanical Damper.

The complete damper assembly forms a linear joint driven by the damper motor through a ball screw to press the movable brake pad against the brake disk. The damper assembly can be further divided in the damping arrangement and damper motor. The damping arrangement is composed of a piston like component (flange) which is attached on the ball screw nut and which slides in a linear bush. To form the linear joint the slider assembly also incorporates by two horizontal guide pins to prevent rotation of the slider. The guide pins are fixed on the cassis plate residing between the slider assembly and the damper motor and they interface with linear busses mounted in guide holes on the flange component. The brake pad is mounted on the slider through a two axis force torque sensor and a flexible component (1mm rubber padding shown here or a flat spring), which provides compliance for better control of the brake clamp force. A thrust bearing takes the reactive axial load due to the normal braking force when operating the

brake disc and prevents axial loading of the damper motor. The damper motor assembly consists of a brushless flat motor (Maxon 30W, EC 45 flat) a magnetic position encoder and a coupler. The customized coupler is used to connect the damper motor shaft to the ball screw and also provides mounting for the ring magnet of the magnetic rotary position encoder. The first actuator prototype is shown in Fig. 4.7.

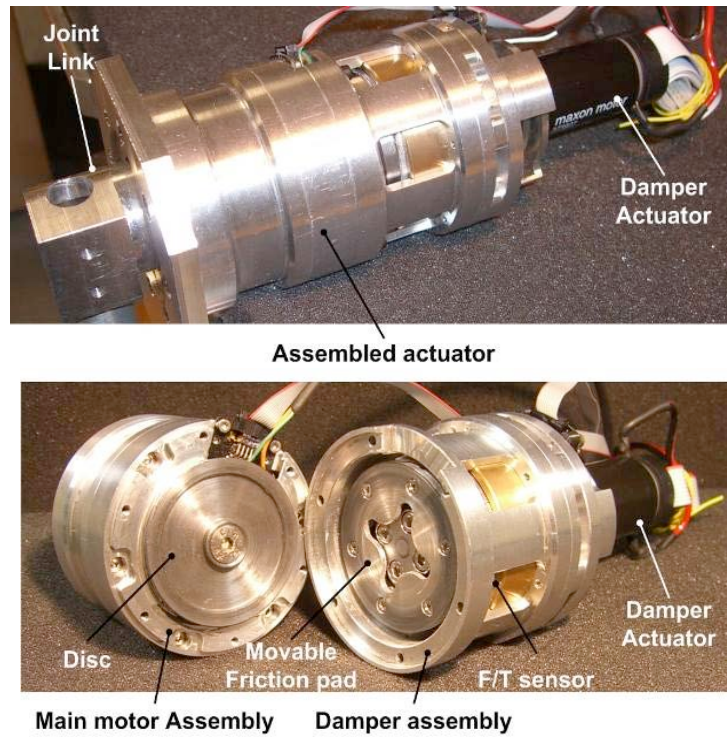
Figure 4.7 The developed variable damping actuator a) the complete assembly b) the main motor assembly exposing the brake disk, c) the damper motor assembly.

The braking mechanism has been designed to apply a braking force up to 500N which provides a braking torque exceeding the stall torque of the motor and is thus suitable also for braking.
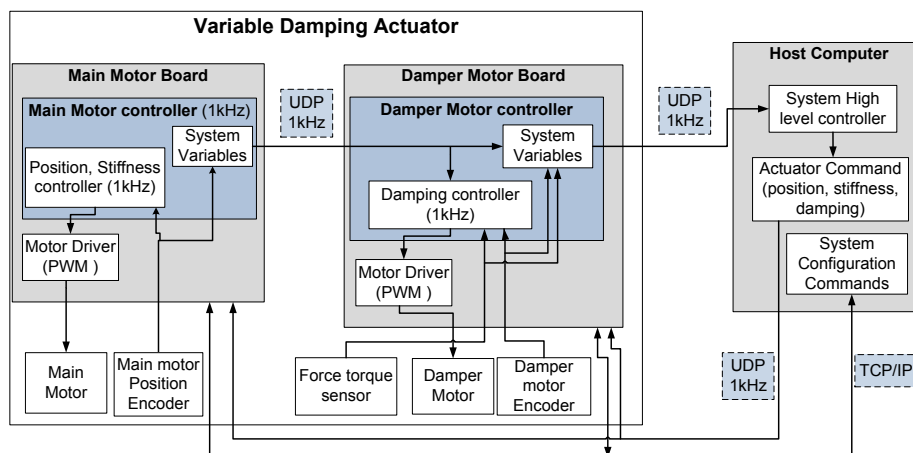

Figure 4.8 Control system architecture.

The actuator control architecture is presented Fig. 4.8. The two actuators are controlled by two dedicated controller boards running 1KHz control loops and communicating over a LAN network. The host computer runs the high level control commanding the position stiffness and damping to the actuator. These commands are transferred through UDP to the two controllers. In this implementation the main motor controller performs the position and stiffness control and passes it system variables to the Damper motor controller which controls damping. Given a value of the wanted damping and using the position and the velocity of the link, control of the damping can be performed using several control strategies:

1. *Through control of the normal force on the disk using the sensor force signal and a friction model of the brake.*
2. *Through control of the applied torque using the sensor torque signal (which is the damping torque during motion).*
3. *Through position control of the damper motor given a friction model of the brake and a stiffness model of the compliant component of the slider assembly.*
4. *A mix of the above.*

The performance of the first prototype of the actuator, Fig. 4.7 [9] was evaluated in a pendulum experiment, Fig. 4.9. The output shaft was connected through a rigid link to a 1kg mass and the mass was allowed to freefall from a high vertical position (180°) and swing until it rested at 0°.
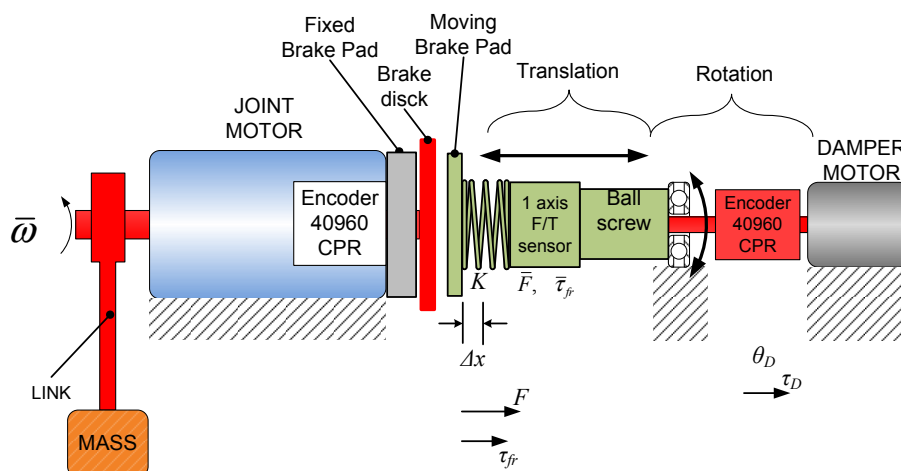
Figure 4.9 Schematic of the actuator evaluation setup.

The performance of the damper motor control is shown in Fig. 4.10. It can be noticed that position tracking is very accurate while also the measured force is also very close to the computed force from the stiffness model. Data for two damping coefficients, namely C1=0.1Nm-s/rad and C2=0.15Nm-s/rad are presented in Fig. 4.11. Finally the ability of the system to achieve the required damping coefficient is demonstrated in Fig. 4.12.
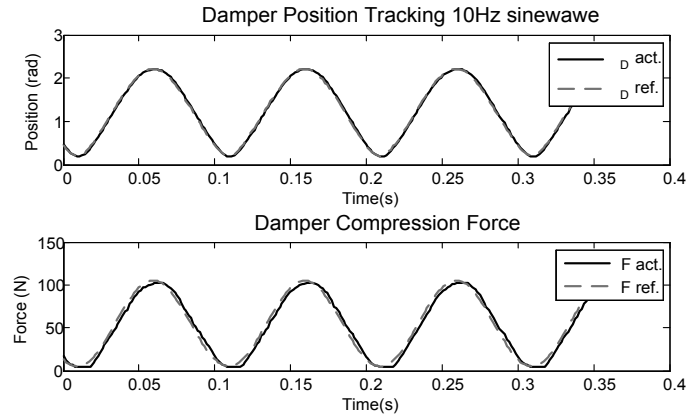
Figure 4.10 Tracking performance of the damper motor.

To validate the design assumptions with respect to the friction properties of the system the μFT coefficient was obtained experimentally during the pendulum experiment. A plot of the measured torque against the measured force, shown in Fig. 2.14, reveals a measured value for friction coefficient μFT_tot which varies in the positive and negative directions. This difference for the two directions could be the result of mechanical misalignments in the assembly but could equally also emanate from sensor nonlinearity in this region.

Figure 4.11 Damper performance plots for a fre falling pendulum mas1kg at 0.2m subjected to damping coefficients C1 and C2.

Figure 4.12 Experimental determination of friction torque coefficient and damping coefficients obtained from the pendulum experiment.

4.3   Revised Motorized linear drive clutch based variable damping mechanism

Following up the development of a first prototype we revised the linear drive based variable damping mechanism by rearranging the two motors to improve compactness and modularity. A schematic of this rearrangement is shown in Fig. 4.13. It employs a Brushless DC motor coupled with a ball screw mechanism to power the actuated brake pad (lower pad in the scheme in Fig. 4.13) of the semi active damper.

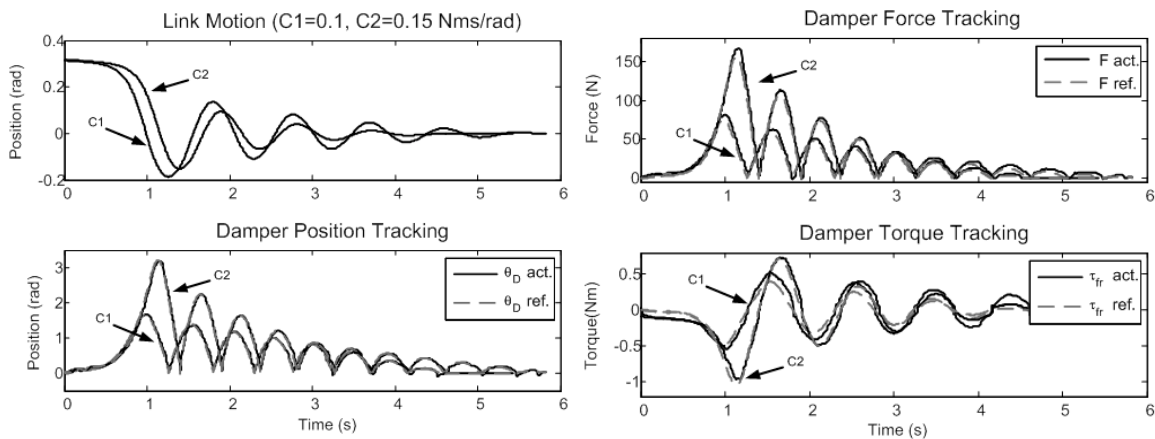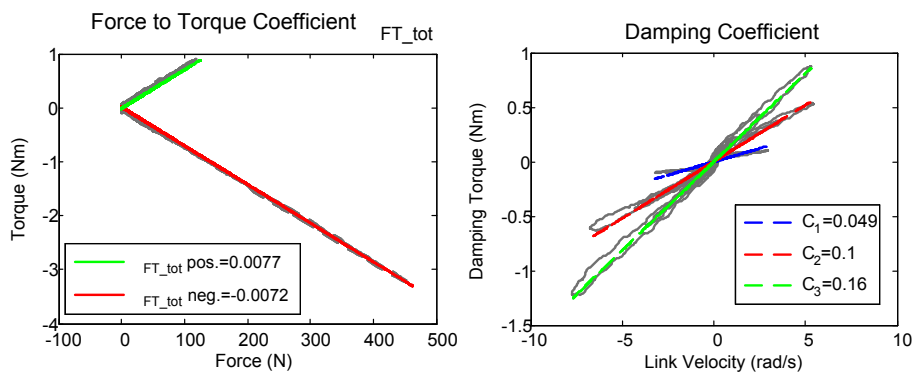The ball screw mechanism is powered by a belt transmission system that allows a substantial reduction of the axial length of the overall system and facilitates the integration of the VPDA in the overall actuator, see Fig. 4.13 and 4.14. A Maxon Brushless DC motor (on the left in Figures 4.13 and 4.14) powers the belt transmission system. The driven pulley is attached to the screw, while the nut is linked to a linear guide formed by two pistons on both sides of the nut, Figure 4.13, 4.14 supported by Teflon bush bearings that exhibit low friction coefficient permitting at the same a more compact integration of the system compared to ball bearing based solutions.

Figure 4.13 Conceptual schematic of the new CompAct™ actuator with variable physical damping.

These pistons act against the extremities of a custom designed leaf spring which is used as series elastic element and force sensor to facilitate the control of the normal force exerted on the frictional surfaces. The system is also equipped with a magnetic encoder which measures the linear displacement of the nut-pistons subassembly by means of a rack and pinion mechanism with an accuracy of 0.55µm, Fig. 2.8. This sensor combination will therefore permit the control of the VPDA in force, position or hybrid mode.

The system is designed to generate a nominal static force of 1kN. An axial ball bearing has been used in this design to support such a relatively high force, Fig. 4.14. The application this normal force nominal value will guarantee a maximum friction torque of approximately 30Nm using a steel against Kevlar fibre based friction material. In such a configuration the VPDA system is capable of generating friction torque that is

comparable to the nominal torque generated by the main actuator motor, i.e. 40Nm. This parameter might be further increased using different friction interfaces that possess higher friction coefficient.
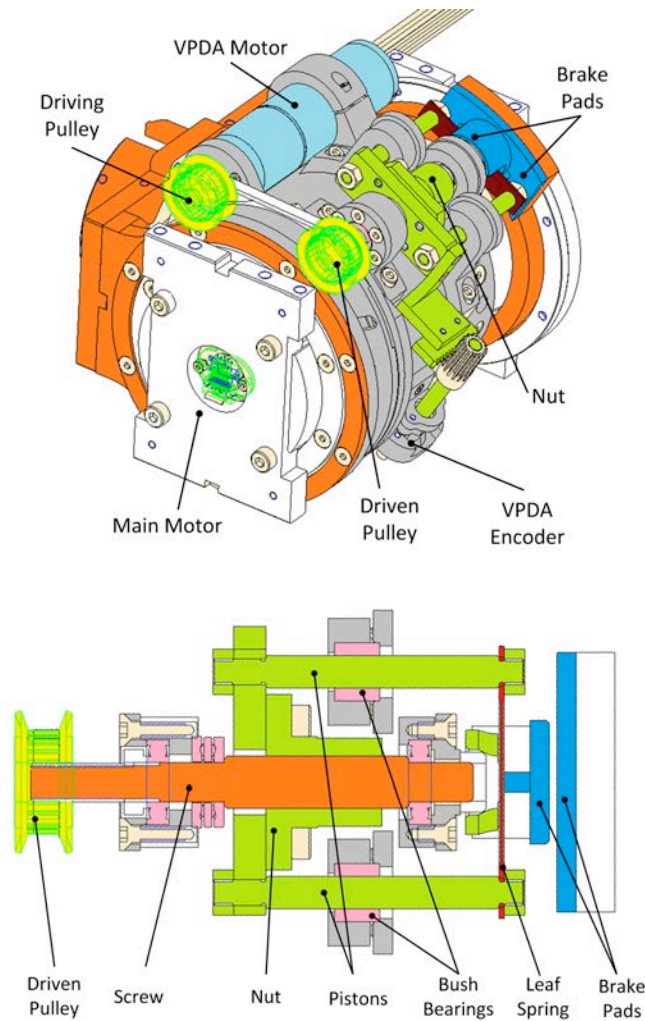

Figure 4.14 CAD design of the whole actuation system and cross section view of the VPDA mechanism subassembly. White: grounded parts; grey: parts fixed to the output of the harmonic drive; orange: parts fixed to the link; green: parts fixed to the nut.

In overall, the other main advantage offered by this solution with respect to the piezo stack actuated version consists in the fact that the stroke of the actuated pad has been increased of several orders of magnitude. This implies two major benefits: relaxation of design tolerances resulting in less expensive design and permits the employment of soft friction material that typically offers higher friction coefficients. On the other hand, the drawbacks of this solution are an increased weight and power consumption. This is because of the addition of the VPDA motor that, differently from piezo actuators, consumes power even during the generation of static force. As an indication on this, we report in Tab. 4.2 the nominal power and weight, respectively.

Table 4.2 Comparison table between motor versions

	Older version (Piezo)	Newer version (Motor+ballscrew)
ΔCost [€]	1400	(-1400)
Normal clutch force [N]	300	1000
Friction torque [Nm]	9	30
Weight [kg]	1.9	2.3
Nominal power [W]	152	242

4.4 Fluid based damper

The fluid based damper is a variable damping actuation unit which produces a damping force proportional to the relative speed, unlike friction dampers (FD), Electroreological (ER), (Magetoreological) MR and the quadratic fluid dampers. The basic goal behind the system development was to obtain a modular damping unit that can be integrated with the VSA-CubeBot system, Fig. 4.15, (e.g. in the shoulder), and change the damping value by changing the fluid chamber area. To deal with these two main features the adopted mechanical solution is inspired by the aperture mechanism, as those used in cameras.
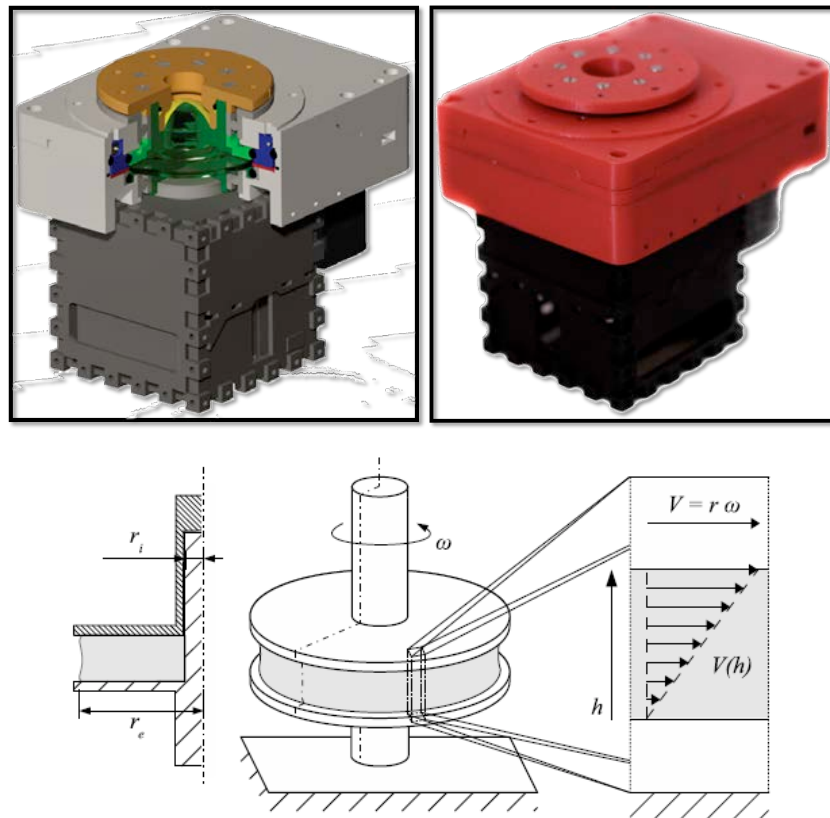

Figure 4.15 Scheme of the variable damper. The meatus has an annular shape, r_i and r_e represent the internal and external radius respectively and h is the height. The relative angular speed of the upper and lower surface is denoted by ω while V represents the linear speed shear of fluid film between two flat discs.

Figure 4.16a shows an exploded view of the variable damping system. The module has two main frames (1 and 15), which implement the connection with the VSA-Cube module, as in Fig. 4.16a, and the integration with the VSA-CubeBot platform as in Fig. 4.16 (b). In particular, the output shaft of the VSA-Cube module is rigidly attached to the rotor of the damping system (8), which is mounted on frames (1) and (15) by two ball bearings. At large flat surface on component (8) creates a shear chamber filled with fluid when the four aperture petals (2) are engaged. Part 7, fixed on the rotor axis, forms another chamber on top of the petals. Along the maximum diameter of (8) and (7), two O-rings (a) and (b) prevent the viscous fluids from leaking from the chambers. The aperture system is actuated by component (3), which is constrained to rotate around its axis, which coincides with rotor axis (8). Part (3) is moved by a wire transmission system (11) actuated by a motor (6) with a pulley (9), fixed on it. Petals (2) are linked to (3) by four pins (12), one for each petal. These pins can translate along prismatic guides grooved on the surface of (1). Part 4closes the aperture system region (through the O-ring c) and realize a hermetic volume. Hence, the viscous fluid is contained in the chamber formed by the inside of rotor 8, and the regions delimited by (1), (8), (4) and (7). The volume inside rotor (8) is closed by a rubber elastic membrane (10), fixed on (8) by the output shaft of the damping system (5), and forms a recovery chamber.
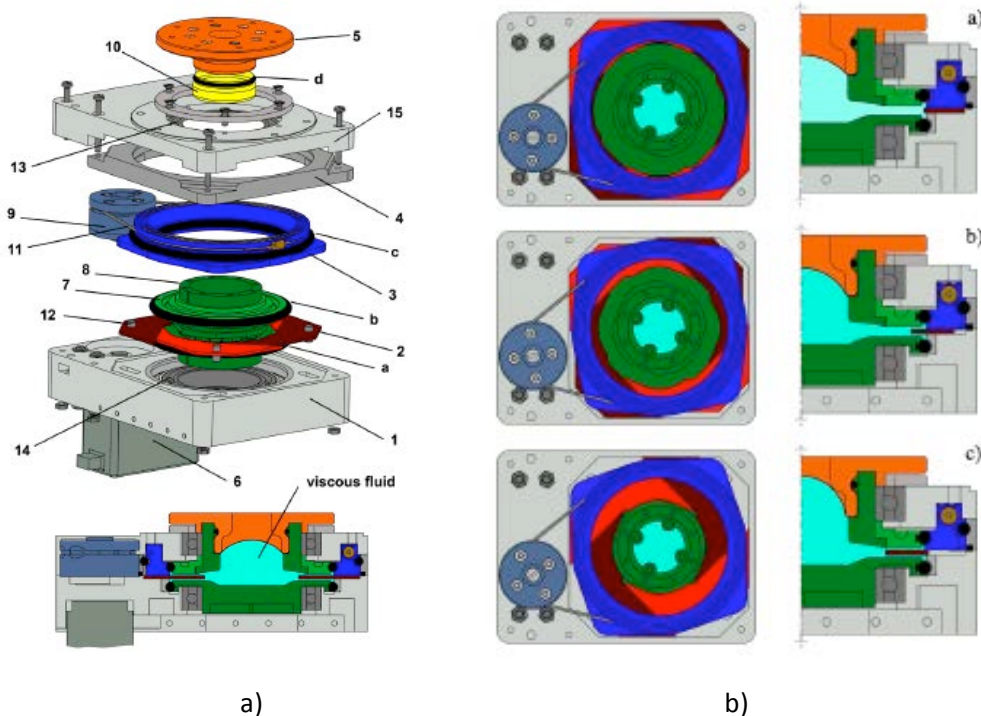

a)   b)

Figure 4.16 a) Exploded 3D view and sec on of the variable damping system with basic components highlighted. The viscous fluid is represented in light blue. The laminar fluid shear is generated between petals 2 and rotors (8) and (7). b) Three different position of the aperture mechanism: a) 0%, b) 20% and c) 100%. During the closure movement petals push the fluid in to the recovery chamber under the rubber membrane. When the system return to 0% closure position the fluid goes out from the recovery chamber and refills recovery chamber.

Figure 4.16b shows three different operating conditions of the damping mechanism. When the system is set to low damping configuration the aperture is completely open and both the chamber and the recovery chamber are filled with fluid. When the aperture system is actuated, petals move inside the rotating chamber pushing the moved fluid inside the recovery chamber in (8). When petals return to an open configuration, the fluid returns from the recovery chamber in (8) to the rotary chamber. The logical scheme illustrating the working principle of the closure mechanism is shown in Fig. 4.17.
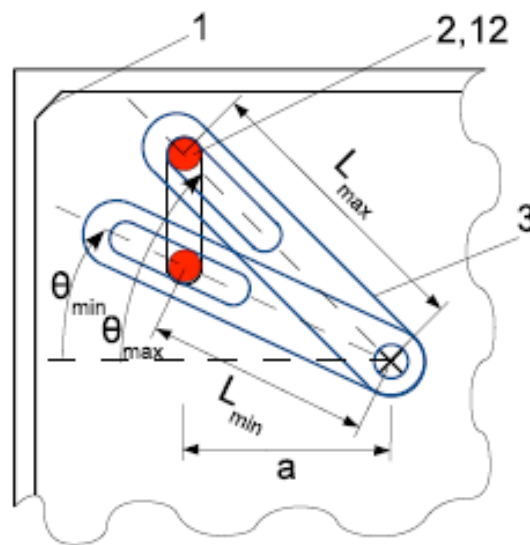

Figure 4.17 Scheme of the aperture mechanism. The blue element represents the element 3, the red element represents one of the petals 12 with the pin 2, and the black element represents the frame 1.

The damper was evaluated with a number of experiments. Results from these experiments are reported in Fig. 4.18 and 4.19. The numerical derivation of data from experiment 1 (Fig. 4.18) is the damping coefficient as a function of velocity as shown in Fig. 41.9. From Fig. 4.18 and 4.19, the range of damping corresponding to different operating conditions can be derived: the damping coefficient ranges from a minimum of 0.15Nms/rad to a maximum of 0.4Nms/rad. Noticeably, a certain amount of hysteresis is present. This hysteresis is, nevertheless, comparable to the hysteresis found in most commercial viscous dampers, which is in the order of 50%. This hysteresis is partially due to the transitory behaviour of the damping fluid which can be characterized from Figure 18. A decay, Fig. 4.20, of about 50% within a time of 6-7 s can be measured. The settling time required to pass from the minimum to the maximum damping value is 0.13.
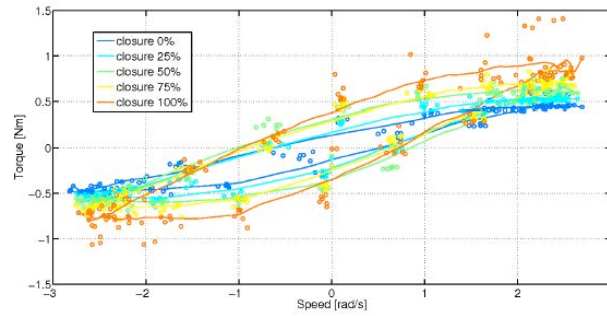
Figure 4.18 Experimental mechanical characteristic of the variable damper. The 5 different colors are obtained for 5 levels of petal closures. The dots are obtained by collecting data during the accelerating and decelerating phases of a periodic sine-wave motion with a period of 2s and a maximum speed of about 2.6rad/s, respectively. The lines are obtained mediating and filtering the dots data.
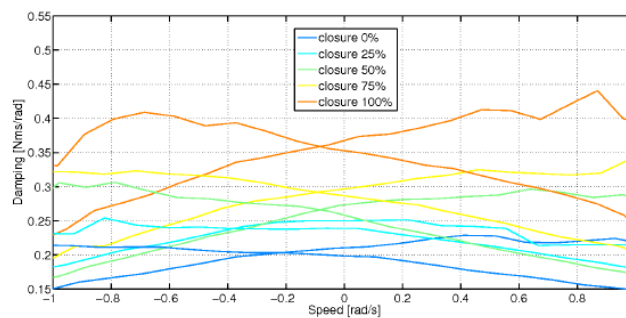

Figure 4.19 Experimental damping for the variable damper, as extracted from data of Fig. 4.18. The two lines of each color are relative to the ascending and descending traits of data in Fig. 4.18. Due to noise in the acquired data, numerical derivation of the mechanical characteristic has been performed just on the central part of the acquired speed range.
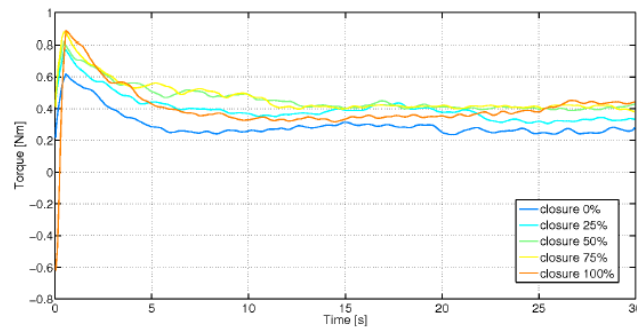

Figure 4.20 Experimental torque decay on the variable damping when continuously opposing to a constant speed of approximately 2.6rad/s. The torque decay is due to natural transitory phenomena inside the damping fluid.

5 References

 [1] M. Catalano, G. Grioli, Manolo Garabini, Felipe Weilemann Belo, Andrea di Basco, N.G. Tsagarakis, A. Bicchi, "A Variable damping module for Variable Impedance Actuation", IEEE International Conference on Robotics and Automation Conference, (ICRA 2012), pp 2666-2672, St Paul, Minnesota.

[2] M. Laffranchi, N. Tsagarakis, and D. Caldwell, "Analysis and development of a semi active damper for compliant actuation systems," IEEE Transactions on Mechatronics, p. PP, 2012.

[3] M. Laffranchi, N. Tsagarakis, and D. Caldwell, "CompactTM arm: a compliant manipulator with intrinsic variable physical damping," in Proceedings of the 2012 International Conference on Robotics, Science and Systems (RSS), Sydney, July 2012.

 [4] Matteo Laffranchi, Lisha Chen, N.G. Tsagarakis, Darwin G. Caldwell, "The Role of Physical Damping in Compliant Actuation Systems , International Conference on Intelligent Robots and Systems (IROS 2012), pp 3079-3085.

 [5] Lisha Chen, Manolo Garabini, Matteo Laffranchi, Navvab Kashiri, N.G. Tsagarakis, Antonio Bicchi, Darwin G. Caldwell, "Optimal Control for Maximizing Velocity of the CompActTM Compliant Actuator", IEEE International Conference on Robotics and Automation, ICRA 2013, pp 516-522.

[6] N. Kashiri, M. Laffranchi, N. G. Tsagarakis, D.G. Caldwell, "On the Stiffness Design of Intrinsic Compliant Manipulators", IEEE Advanced Intelligent Mechatronics, AIM 2013, pp 1306-1311.

[7] N. Kashiri, M. Laffranchi, N. G. Tsagarakis, I. Sardellitti, D.G. Caldwell, "Dynamic Modeling and Adaptable Control of the CompActTM Arm", IEEE International Conference on Mechatronics, ICM 2013, pp 477-482.

[8] L. Chen, M.Laffranchi, J. Lee, N. Kashiri, N.G.Tsagarakis, D.G. Caldwell, "Link Position Control of a Compliant Actuator with Unknown Transmission Friction Torque", IEEE International Conference on Intelligent Robots and Systems (IROS), 2013, pp 4058-4064.

[9] Ioannis Sarakoglou, N.G. Tsagarakis, Yogesh karandikar, Darwin G. Caldwell, „Development of a Hybrid Actuator with Controllable Mechanical Damping", accepted to ICRA 2014.